Characterization of the Reduced and Oxidized Polypyrrole/Water Interface: A Molecular Dynamics Simulation Study

J. J. López Cascales,* A. J. Fernández, and T. F. Otero

Laboratory of Electrochemistry, Intelligent Materials and Devices (CEMI), Ingenieros Industriales, Campus de Alfonso XIII, Univeridad Politécnica de Cartagena, 30201 Cartagena, Murcia, Spain

Received: December 14, 2002; In Final Form: June 12, 2003

To simulate the processes that take place at the polypyrrole/water interface under different states of oxidation of the polymer, a reliable model of the polymer/water system is necessary. To this end, a model with atomic detail of the polypyrrole/water system was simulated for first time in both the oxidized (charged) and reduced (uncharged) polymer. The system consists of a single layer of water molecules between two layers of polypyrrole film. Each polymer film was formed of 64 polymeric chains of 10 monomeric units each, and after oxidation of each polypyrrole chain, 128 chloride ions were included to maintain the electroneutrality of the system. In this way, a classical molecular dynamics simulation was carried out for both oxidized and reduced polypyrrole. From the simulated trajectories, macroscopic properties, such as the polypyrrole density in its reduced state and polymer swelling after oxidation, were simulated. Thus, valuable information related to the atom distribution profile and water and counterion permeation across the polymer/water interface was obtained. In this regard, due to the high hydrophobicity of the reduced polypyrrole, water molecules were repelled from the core of the polymer matrix and so did not penetrate into the polymer matrix, at least during our simulations. As a consequence of this hydrophobicity, a sharp polymer/water profile was obtained. In the case of the oxidized polypyrrole, chloride ions penetrated into the core of the polymer matrix to keep the electroneutrality of the system. As a result of this ion penetration into the polymer and the strong polymer−polymer repulsions between charged sites inside the oxidized polypyrrole, a swelling of the polymer matrix of 11% was measured, while the thickness of the polypyrrole/water interface increased by 50% compared with its reduced state. Finally, charge distribution and electric potential profiles across the polypyrrole/water interface were obtained in both oxidized and reduced states. The contribution of water to the electric potential which consists of reorientating its dipoles was measured in both states.

1. Introduction

The electrochemical behavior and electrochemical properties of polypyrrole, as a soft, wet, and amorphous material, have been widely studied due to the wide range of electrical,[1] mechanical,[2] optical,[3] and sensing[4] properties, which can be controlled electrochemically.[5] Most of these properties are related to oxireduction processes, where the polymer changes reversibly from a neutral (reduced) to an oxidized (charged) state. During this process, the electrolyte plays a crucial role, counterions penetrating the polymer to maintain the electroneutrality of the system. As a result of this oxireduction process, important structural changes take place in the polymer, which passes from a neutral and compact state (reduced state) to a gel state (oxidized state)[6] because the polymer matrix swells during oxidation, as water and counterions penetrate into the polymer matrix.

Alongside other conducting polymers, such as polythiophene and polyaniline, polypyrrole is one of the most studied of conducting polymers, mainly due to its high stability in both water and organic solvents. It is a fact that most of its technological applications, such as *artificial muscles*,[4] require aqueous media that has led us to focus our interest on this system.

Much effort has gone into studying the amorphous structure of polypyrrole using X-ray photoelectron spectroscopy (XPS),[7] atomic force microscopy (AFM),[8,9] and electrochemical techniques.[6,10,11] However, little attention has been paid to the structure of the polypyrrole/water interface, even though most of the above-mentioned technological applications are associated with oxireduction processes in the wet state. This lack of information seems to be related to the serious technical and theoretical difficulties involved in measuring this amorphous part of the system. In this setting, molecular dynamics simulations emerged as a successful technique for the study of a vast number of systems[12−14] in atomic detail. Thus, for example, Gomes et al.[15] studied the transport of calcium ion through the water/nitrobenzene interface; Kirkpatrick et al.[16] studied the bonding of chloride ions to different types of interfaces, and Berendsen et al.[17] studied a phospholipid/water interface and its properties.

Our aim, described in this paper, was to study the polypyrrole/water interface by following a procedure similar to those applied in the literature to other interfaces involving aqueous systems, such as lipid membranes.[18−21] The first section will be devoted to introducing the model and those parameters used in our simulations. We then validate our simulations by reference to some experimental results available in the literature. Finally, some results concerning atom distribution profiles, electric

* To whom correspondence should be addressed. E-mail: javier.lopez@upct.es.

10.1021/jp027717o CCC: $25.00
Published on Web 08/05/2003

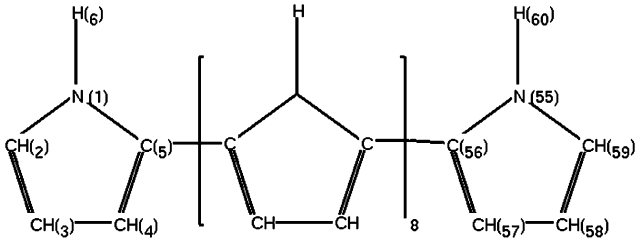

Figure 1. Polypyrrole atom numeration in its reduced state. The same numeration has been employed in its oxidized state

charge distributions, and electric potentials across the interface will be presented in atomic detail for both reduced and oxidized polypyrrole.

2. Method and Models

A periodical three dimension box of $V_x^0 = 7$, $V_y^0 = 7$, and $V_z^0 = 5$ nm was generated as follows: Two amorphous polymeric layers containing 64 polypyrrole molecules of 10 monomeric units each (Figure 1) were randomly placed perpendicularly to the polymer layer. This polypyrrole unit was built using the commercial package HyperChem.[22]

Although recent years have seen the development of new models of water, in which the polarizability of the water molecules is presented,[23−25] the SPC model (single point charge)[26] was used in our simulations. A single layer of 1.6 nm thickness between the two polypyrrole layers was filled with water by replication of a single and equilibrated box of water at 298 K of homogeneous density and containing the 216 water molecules of the SPC model. A previous article[19] described how an aqueous layer of 1 nm thickness was sufficient to remove all the simulation artifacts between both sides of the charged layers, giving a bulk behavior of the water in the middle of this layer. A total of 2677 water molecules were required to fill up the gap existing between both polymer layers. So, the total number of atoms in our system was 15 711.

For the oxidized polypyrrole system, 128 chloride ions, Cl^-, were introduced into the above computing box to preserve the electroneutrality of the oxidized system, due to the fact that a net charge of +1 was placed on each oxidized polypyrrole polymer chain. In this sense, 128 water molecules were substituted by 128 Cl^- anions, following the principle of minimizing the electrostatic energy of the system. This system was therefore constituted by 15 455 atoms in total. Two snapshots of both systems (reduced and oxidized polypyrrole and water) are displayed in Figures 2 and 3.

The atomic charge distribution (Table 1) on each single polypyrrole molecule was calculated by the CNDO quantum mechanical method.[27] To bring the system to a steady state, the atomic charges on the polypyrrole and counterions were reduced by a factor of 2, a reduction that has been shown to be effective in the simulation of soap/alcohol/water interfaces,[28] biological membranes,[17] and micelles.[29] The physical justification for this reparametrization is, in short, that Coulomb interactions in the system are exaggerated due to the insufficient screening performance of the SPC water molecules. In the simulation, a relative dielectric constant of 1 is used while electronic polarizations are neglected.

As regards the distribution of atom charges in the oxidized polypyrrole, we distributed the net positive charge between three monomeric units (monomers 4−6), which were constrained to the same plane. This model is based on experimental evidence[30,31] in which the positive charge in the oxidized polypyrrole was distributed between 3 and 4 rings of a polypyrrole chain.

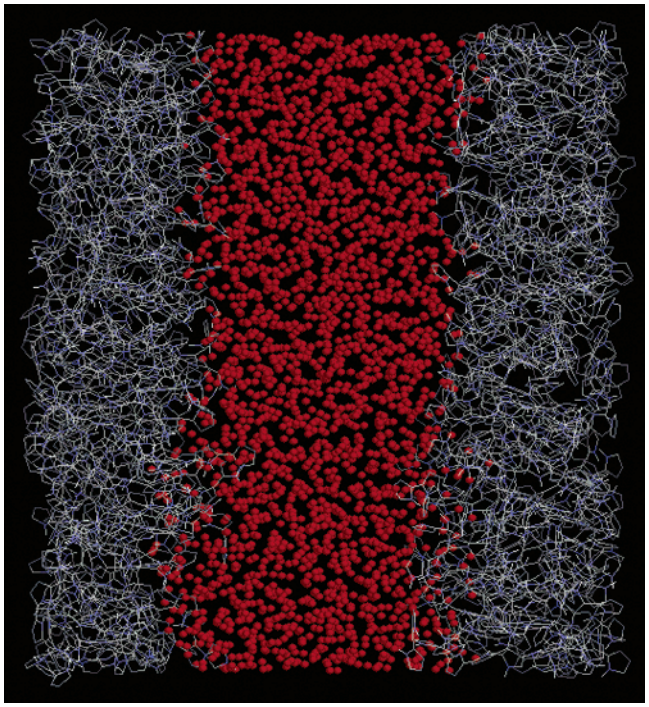

Figure 2. Snapshot of the system during the simulation composed of 128 reduced polypyrrole molecules (64 polypyrrole molecules on each of the two layers of polypyrrole) and 2677 water molecules. The red beads correspond to the oxygen of each water molecule.

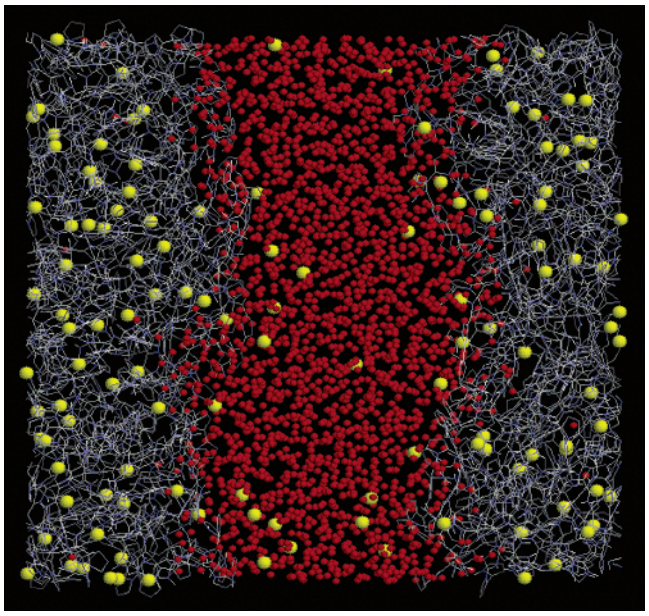

Figure 3. Snapshot of the system during the simulation composed of 128 oxidized polypyrrole molecules (64 polypyrrole molecules on each of the two layers of polypyrrole), 128 chloride ions, and 2549 water molecules. The red and yellow beads correspond to the oxygen of each water molecule and to the chloride ions, respectively.

The atomic distances and covalent angles proposed by GROMOS[32] were corrected by the values obtained by Kofranek et al.[33] using ab-initio calculation.

Thus, both layers of the reduced and oxidized polypyrrole were set to resemble an amorphous polymer film. The full system was subjected to a steepest descendent energy minimization step to remove the excess of energy from the system, by using the GROMOS[32] force field. Lennard-Jones and dihedral

TABLE 1: Polypyrrole Atomic Charge Distribution in Its Oxidized and Reduced State, in e⁻ Units

reduced polypyrrole		oxidized polypyrrole	
atom number	charge (e⁻)	atom number	charge (e⁻)
1, 7, 13, 19, 25, 31, 37, 43, 49, 55	−0.08	1, 7, 13, 37, 43, 49, 55	−0.08
2, 8, 14, 20, 26, 32, 38, 44, 50, 56	0.04	2, 8, 14, 38, 44, 50, 56	0.04
3, 9, 15, 21, 27, 33, 39, 45, 51, 57	−0.05	3, 9, 15, 39, 45, 51, 57	−0.05
4, 10, 16, 22, 28, 34, 40, 46, 52, 58	−0.05	4, 10, 16, 40, 46, 52, 58	−0.05
5, 11, 17, 23, 29, 35, 41, 47, 53, 59	0.04	5, 11, 17, 41, 47, 53, 59	0.04
6, 12, 19, 24, 30, 36, 42, 48, 54, 60	0.1	6, 12, 19, 42, 48, 54, 60	0.1
		19, 31	0.27
		25	0.28
		20, 26, 32	0.02
		21, 27, 33	0.00
		22, 28, 34	0.00
		23, 29, 35	0.02
		24, 30, 36	0.02

angle parameters were taken from the standard GROMOS force field without further modification.

During our simulations, a time step of 1 fs was used. Longer time steps rendered the simulations unstable. Two different spherical cutoffs[12] were used to compute the nonbounded forces (electrostatic and van der Waals): a short cutoff of 1 nm and a long cutoff of 1.8 nm. We wish to emphasize the importance of choosing the correct short cutoff to avoid unstable simulation and to prevent the system from drifted apart toward unpredictable results.[13,34] The neighbor list was updated every 10 time steps of the simulation[12,32] as in previous articles.[18,35] The interactions of the atoms lying within the short cutoff were computed every time step, while those of the atoms lying between the long and the short cutoff were computed only for the first time step since they remained more or less constant during the following nine time steps. Nonbounded forces beyond the long cutoff were neglected. Bond lengths were constrained by SHAKE algorithm,[36] with a tolerance of 0.0001 nm.

In both cases, the whole system was coupled to an external pressure and temperature bath[37] of 1 atm and 300 K, with coupling constants of $\tau_P = 0.5$ ps and $\tau_T = 0.1$ps, respectively. Due to the anisotropy of the system, each of the edges of the periodical three-dimensional box was independently coupled to the pressure bath.

To ascertain whether the system was nearing an equilibrated state, the volume of the computing box was monitored as in previous articles.[18,19] In both cases (oxidized and reduced state), the first 500 ps of simulations were discarded during the equilibration of the system and the analysis was performed over the following 1000 ps. The dimensions of the computing boxes (in nm) were the following: $V_x = 5.91 \pm 0.06$, $V_y = 6.06 \pm 0.03$, and $V_z = 5.592 \pm 0.006$ for the reduced state and $V_x = 5.54 \pm 0.11$, $V_y = 5.75 \pm 0.11$, and $V_z = 6.73 \pm 0.14$ for the oxidized state.

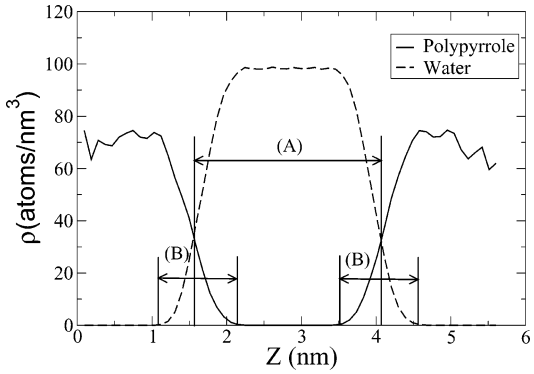

Figure 4. Atom distribution along the normal axis (*z*) to the polymer−water interface: Reduced state. Distance A represents the thickness of the water layer used to compute the polymer density (see text), and distance B represents the thickness of the polypyrrole/water interface.

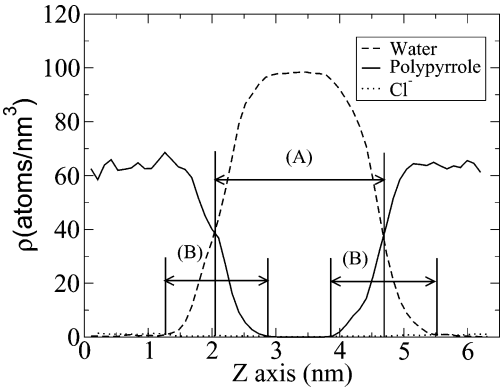

Figure 5. Atom distribution along the normal axis (*z*) to the polymer−water interface: Oxidized state. Distance A represents the thickness of the water layer used to compute the polymer density (see text), and distance B represents the thickness of the polypyrrole/water interface.

3. Results and Discussion

3.1. Interface Atom Distribution. Atomic distributions across the polypyrrole/water interface can be obtained from the simulated trajectories, Figures4 and 5. From these figures, the shape and thickness of the polymer/water interface in their oxidized and reduced states can be estimated.

From Figures 4 and 5 we observe how, even when the size of the system was limited (total number of atoms in the system), a plateau for the atom distribution profile between both interfaces for the different components of the system. This means that the samples obtained from a combination of the system size and trajectory length were large enough to provide a statistical study of the different properties related to these systems (oxidized and reduced).

From the atomic distributions, the macroscopic density of the polymer can be estimated and the value attained can be used to check the validity of the simulations. Considering the volume occupied by the polypyrrole as the total volume of the computing box minus the volume occupied by the water layer (assuming a thickness of 2.5 nm for the water layer as the distance between the intersection of the polymer/water profiles between both interfaces, such as in Figure 4), a density of 1.47 g/cm^3 was estimated from our simulations. This result overlaps experimental values[38,39] which range from 1.47 to 1.51 g/cm^3.

Furthermore, from the atom distribution function, a sharper polypyrrole/water interface is observed in the reduced state (Figure 4) than in the oxidized state (Figure 5). The oxidized polymer/water interface is roughly 50% thicker than that of the

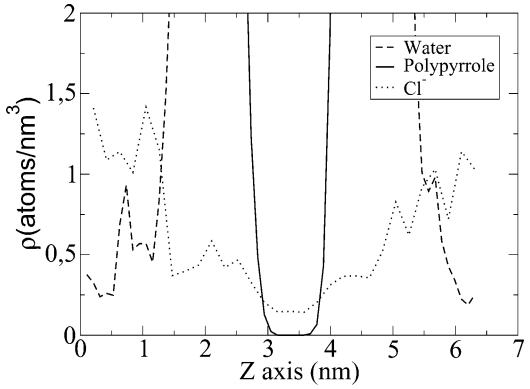

Figure 6. Amplification of the atom distribution profile along the normal axis (z) to the polymer−water interface: Oxidized polymer.

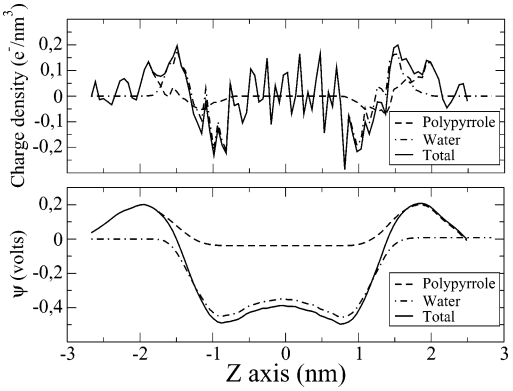

Figure 7. Charge density and electric potential across the polymer/water solution interface in the reduced state. Zero was placed at the middle of the computing box.

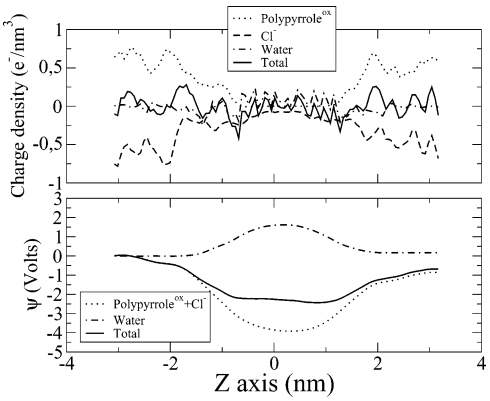

Figure 8. Charge density and electric potential across the polymer/water solution interface in its oxidized state. Zero was placed at the middle of the computing box.

reduced state. The thickness of the interface was defined as the distance between the polypyrrole and water profiles when each of them is extinguished at each interface, as can be seen in Figures 4 and 5. This is clear evidence of the important changes taking place in the molecular interactions. Thus, in the polypyrrole reduced state, polymer−polymer interactions prevail over the polymer/water interactions mainly due to the high hydrophobicity of the reduced polymer, while the oxidized state induces much more favorable polymer/water interactions due to the strong electrostatic interactions that take place between the charged polymer and the counterions. In other words, the high hydrophobicity of the reduced polymer expells the water molecules from the bulk polymer along the simulated trajectory, leading to sharply defined polypyrrole/water interface than in the oxidized state. Figure 5 shows a more diffuse polymer−water interface. The structure of the oxidized film is close to that of a gel as was suggested by Otero et al.,[6,10] in which chloride ions penetrate into the bulk of the oxidized polypyrrole (Figure 6) to balance the charge, losing part of their hydration shell as they do so. Figure 6 corresponds to an amplification of the atom distribution across the oxidized polymer/water interface, which clearly shows the dehydration of the counterions as they penetrate the polymer matrix, mainly due to the high hydrophobicity of the environment inside the polypyrrole, as was suggested by an anonymous reviewer of this manuscript. This progressive loss of the chloride hydration shell can be observed very easily from a video movie[40] produced from the simulated trajectory.

Penetration of water into the polypyrrole dragged by the counterions has been experimentally observed[6,41] from the swelling of the polymer matrix. From our simulations, we are able to evaluate the percentage of swelling from the difference between the atomic polymer densities of the oxidized and reduced state. A density of 70 atoms/nm^3 was estimated for its reduced state and 63 atoms/nm^3 for the oxidized polymer; a swelling of 11% was obtained for the oxidized polymer with respect to the reduced state, in a good agreement with experimental results[42] where a range of 3−30% has been measured. This wide range of values is related to the thickness of the polypyrrole film and the level of oxidation in the polymer.

3.2. Charge and Electric Potential across the Polymer/Water Interface. As a consequence of the atom distribution across the polypyrrole/water interface, an electric field is obtained across the interface in both the oxidized and reduced states.

Figures 7 and 8 show the atom charge distribution (expressed in e$^-$/nm^3) across the interface for both systems. In the reduced state, the anisotropic orientation of the water dipoles introduces a certain charge density into the polymer very close to the interface. This is caused by the orientation of the existing dipoles of the monomeric units of the polypyrrole chains to minimize the energy of the system. This anisotropic orientation of water becomes zero near the bulk water zone, as is observed from the water charge distribution profile (Figure 7).

In the case of oxidized polypyrrole, the net charge anchored on the polymer is clearly compensated by chloride ions (Cl^-): the charge distribution associated with chloride ions is almost a mirror image of the polypyrrole distribution. As regards water, its contribution to the net charge is not so noticeable as in the reduced state, although it does compensate the excess of charge in the vicinity of the polymer interface.

In addition to the electric charge distribution, the electrostatic potential, ψ, can also be computed from the simulation by mean of a numerical evaluation of the double integral of the charge density (ρ)[43] as follows:

$$\psi(z) - \psi(0) = -\frac{1}{\epsilon_0}\int_0^z dz' \int_0^{z'} \rho(z'')\, dz''' \qquad (1)$$

Here the origin of z is taken at the middle of the polymer film. By using this method, we are able to indivually estimate the contribution of each one of the separate components of the system: polypyrrole, water, and counterions. We are aware that electrostatic potential computed in this way is consistent with the computed charge density using Poisson's equation, without using a cutoff radius. However, it should be noted that small discrepancies emerged between both symmetric sides of the system (they do not even look like mirror images) due to the

propagation of small errors of integration toward the upper integration limit and due to the limited sampling of the system.

The contributions of each component to the total electrostatic potential are depicted in Figures 7 and 8. As regards the reduced polypyrrole film, the contribution of water presents a value of around −0.5 V in bulk water, a value that agrees quite well with the results obtained by van Buuren et al.[43] for the contribution of water to the electric potential in an oil/water interface.

On the other hand, in the oxidized polypyrrole/water interface, water contributes to the total electric potential in an opposite way to the above, reaching a potential of around 3 V in the middle of the water layer. This noticeable difference in the net water contribution to the total potential is obviously due to contribution of the polypyrrole + chloride that tries to minimize this excess of potential by changing the orientation of water dipoles. Finally, a net potential of −2 V was attained from simulations for the net potential in bulk water of the oxidized system.

4. Conclusions

We have simulated for first time the polypyrrole/water interface in atomic detail in both oxidized and reduced polypyrrole state.

Valuable macroscopic information, such as the density of the reduced polypyrrole and the swelling percentage of polypyrrole when it changes its oxidation state, has been successfully reproduced. Thus, the density of 1.47 g/cm^3 calculated was in good agreement with experimental data and an 11% swelling of the polymer matrix was measured from the simulation when polypyrrole was oxidized.

In addition, insight into the atom distribution profile, thickness of the polypyrrole/water interface, and electric potential across the interface has been gained for both reduced and oxidized polypyrrole. Thus, we found that the oxidized polypyrrole/water interface is around 50% thicker than the reduced polypyrrole/water interface. We also found that chloride ions lose their hydration shell when they penetrate into the oxidized polypyrrole matrix from the bulk water to balance the excess charge inside the polymer.

Further studies concerning the solubility of different counterions inside the polypyrrole matrix, the dynamic properties of water in the polypyrrole/water interface, and related topics are under development.

Acknowledgment. The authors acknowledge the financial support from the Spanish Government and from the SENECA Foundation through the Projects BQU-2001-0477 and AR-8-02710/FS/02, respectively. We also acknowledge to the Computing Center Staff of the Polytechnic University of Cartagena their efforts in carrying out the simulations on which this article is based. Finally, we wish to thank the anonymous reviewers of this manuscript for their valuable comments which have permitted us to make this work more easily understood.

References and Notes

(1) Otero, T. F.; Cantero, I.; Grande, H. *Electrochem. Acta* **1999**, *44*, 2053.

(2) Roemer, M.; Kurzenknabe, T.; Oesterschulze, E.; Nicoloso, N. *Anal. Bioanal. Chem.* **2002**, *8*, 754.

(3) Otero, T. F.; Bengoechea, M. *Langmuir* **1999**, *15*, 1323.

(4) Otero, T. F.; Cortes, M. T. *Adv. Mater.* **2003**, *3*, 279.

(5) Otero, T. F. In *Modern aspects of electrochemistry*; White, R. E., Ed.; Kluwer Academic: Dordrecht, The Netherlands, 1999; pp 307−434.

(6) Otero, T. F.; Grande, H.; Rodríuez, J. *Phys. Chem. B* **1997**, *19*, 3688.

(7) Girotto, E. M.; Gazotti, W. A.; Tormena, C. F.; De Paoli, M. A. *Electrochim. Acta* **2002**, *47*, 1351.

(8) Miles, M. J.; Smith, W. T.; Shapiro, J. S. *Polymer* **2000**, *41*, 3349.

(9) Idla, K.; Talo, A.; Niemi, H. E. M.; Forsen, O.; Ylasaari, S. *Surf. Interface Anal.* **1997**, *11*, 837.

(10) Otero, T. F.; Grande, H.; Rodriguez, J. *Electrochim. Acta* **1996**, *11*, 1863.

(11) Miller, D. L.; Bockris, J. O. *J. Electrochem. Soc.* **1992**, *4*, 967.

(12) van Gunsteren, W. F; Berendsen, H. J. C. *Angew. Chem., Int. Ed. Engl.* **1990**, *29*, 992.

(13) Frenkel, D.; Smit, B. *Understanding Molecular Simulations*; Academic Press: San Diego, CA, 2002.

(14) Rapaport, D. C. *The art of molecular dynamics simulations*; Press Syndicate of the University of Cambridge: Cambridge, U.K., 2002.

(15) dos Santos, D. J. V. A.; Gomes, J. A. N. F. *ChemPhysChem* **2002**, *3*, 946.

(16) Kalinichev, A. G.; Kirkpatrick, R. J. *Chem. Mater.* **2002**, *14*, 3539.

(17) Egberts, E.; Marrink, S. J.; Berendsen, H. J. C. *Eur. Biophys. J.* **1994**, *22*, 423.

(18) López Cascales, J. J.; García de la Torre, J.; Marrink, S. J.; Berendsen, H. J. C. *J. Chem. Phys.* **1996**, *7*, 2713.

(19) López Cascales, J. J.; Berendsen, H. J. C.; García de la Torre, J. *J. Phys. Chem.* **1996**, *21*, 8621.

(20) López Cascales, J. J.; Huertas, H. L.; García de la Torre, J. *Biophys. Chem.* **1977**, *69*, 1.

(21) López Cascales, J. J.; García de la Torre, J. *Biochim. Biophys. Acta* **1997**, *1330*, 145.

(22) *HyperChem*; package developed by and licensed from HyperCube, Inc., 1992.

(23) Stuart, S. J.; Berne, B. J. *J. Phys. Chem.* **1996**, *100*, 11934.

(24) Levitt, M.; Hirshberg, M.; Sharon, R.; Laiding, K. E.; Daggett, V. *J. Phys. Chem. B* **1997**, *101*, 5051.

(25) Oyen, E.; Hentschke, R. *Langmuir* **2002**, *18*, 547.

(26) Berendsen, H. J. C.; Postma, J. P. M.; van Gunsteren, W. F.; Hermans, J. In *Intermolecular forces*; Pullman, B., Ed.; Reidel: Dordrecht, The Netherlands, 1981; p 331.

(27) Pople, J. A.; Segal, G. A. *J. Chem. Phys.* **1966**, *44*, 3289.

(28) Egberts, E. Molecular Dynamics Simulation of Multibilayer membranes. Ph.D. Thesis, Rijkuniversiteit Groningen: Groningen, The Netherlands, 1988.

(29) Jonsson, B.; Edholm, O.; Teleman, O. *J. Chem. Phys.* **1986**, *85*, 2259.

(30) Maller, A. M.; Compton, R. G. *J. Chem. Soc., Faraday Trans.* **1989**, *85*, 977.

(31) Asavapiriyanont, S.; Chandler, G. K.; Gunawardena, G. A.; Pletcher, D. *J. Electroanal. Chem.* **1984**, *177*, 229.

(32) van Gunsteren, W. F.; Berendsen, H. J. C. *GROMOS: GROningen MOlecular Simulation Software Package*; Biomos: Nijenborgh 4, 9747AG Groningen, The Netherlaands, 1987.

(33) Kofranek, M.; Kovás, T.; Karpfen, A.; Lischka, H. *J. Chem. Phys.* **1992**, *6*, 4464.

(34) Steinbach, P. J.; Brooks, B. R. *J. Comput. Phys.* **1994**, *15*, 667.

(35) Egberts, E.; Berendsen, H. J. C. *J. Chem. Phys.* **1988**, *89*, 3718.

(36) van Gunsteren, W. F.; Berendsen, H. J. C. *Mol. Phys.* **1977**, *34*, 1311.

(37) Berendsen, H. J. C.; Postma, J. P. M.; van Gunsteren, W. F.; DiNola, A.; Haak, J. R. *J. Chem. Phys.* **1984**, *8*, 3684.

(38) García-Camamero, E.; Arjona, F.; Guillén, C.; Fatás, E.; Montemayor, C. *J. Mater. Sci.* **1990**, *25*, 4914.

(39) Genies, E. M.; Bidan, G.; Diaz, A. F. *J. Electroanal. Chem.* **1983**, *149*, 101.

(40) López Cascales, J. J. *Videomovie: Computer Simulations of the polypyrrole/water interface*; 2003. To get a free copy of this, please contact javier.lopez@upct.es or the editor of JPC or download it from the website http://www.upct.es/electroquimica/laboratorio/javierc.htm

(41) Suarez, M. F.; Compton, R. G. *J. Electroanal. Chem.* **1999**, *2*, 211.

(42) Smela, E.; Gadegaard, N. *J. Phys. Chem. B* **2001**, *39*, 9395.

(43) van Buuren, A. R.; Berendsen, H. J. C. *Langmuir* **1994**, *10*, 1703.